3 TD-PEEM Kinetics studies*

This section deals with the question to what extent it is possible to interpret the PEEM intensity as a measure of the absolute adsorbate coverage. These results are going to be extensively employed in the following. Difficulties arise when the measured PEEM intensity variation of the Pt(110) surface upon CO exposure, shown in Fig. 3.1a, is compared with a Kelvin probe data, e.g., by Freyer and coworkers [1] shown in Fig. 3.1b. While the PEEM intensity monotonically decreases by increasing the CO exposure, implying an increase of the WF, in the Kelvin probe experiment the WF changes are initially negative, until at a $2 \cdot 10^{-6}$ mbar·s the trend is reversed. Imbihl and coworkers observed a similar initial decrease, albeit of only 40 mV [2].

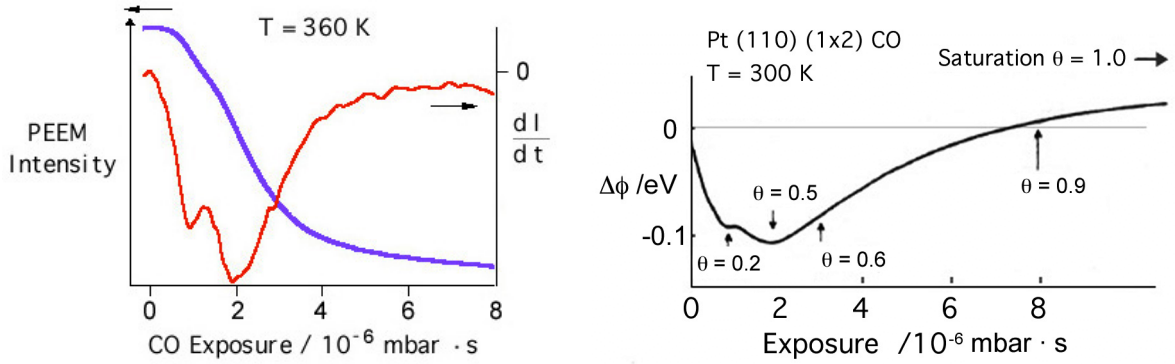

Fig. 3.1 a) The variation of the PEEM intensity upon CO exposure; b) Kelvin probe WF data.

Recalling the Fowler relation described in Section 2.1, the derivative of the PEEM intensity with respect to the exposure yields the inverse of the derivative of the WF in respect to the coverage. Quite remarkably, the first derivative of the PEEM intensity shows a close resemblance with the WF measurement recorded by the Kelvin probe. To our knowledge, no explanation of this effect has been proposed. It has been observed [3], however, that in contrast to other methods the PEEM could be affected not only by changes of the WF but possibly even by modification of the DOS of the electrons in the Pt. And indeed, quite dramatic modifications are apparent in the CO/Pt(110) system, as shown in Fig. 1.5.

* References at page 35

Nonetheless, measurements of the PEEM intensity in dependence of temperature seem to agree with previous Kelvin Probe data of M. Eiswirth [4] and Comrie and Lambert [5], who found a 150 mV increase of the WF upon saturation. As shown in Fig. 3.2, by cooling the Pt(110) sample in the presence of CO, the PEEM intensity begins to decrease at 530 K, when CO adsorption sets in. At 430 K it reaches a minimum and increases again by lowering the temperature before reaching a constant value around 370 K. This inversion of the contrast can be explained by the decrease of the total dipole moment of the surface at high CO coverages, at conditions where the dipoles substantially interact with their neighbors. The modulation of the CO partial pressure has been employed to study the relative phase between PEEM intensity and CO pressure. While between 450 and 580 K the two signals are in antiphase, they become in phase at lower temperatures (which corresponds to higher coverages), confirming the existence of the two different regimes.

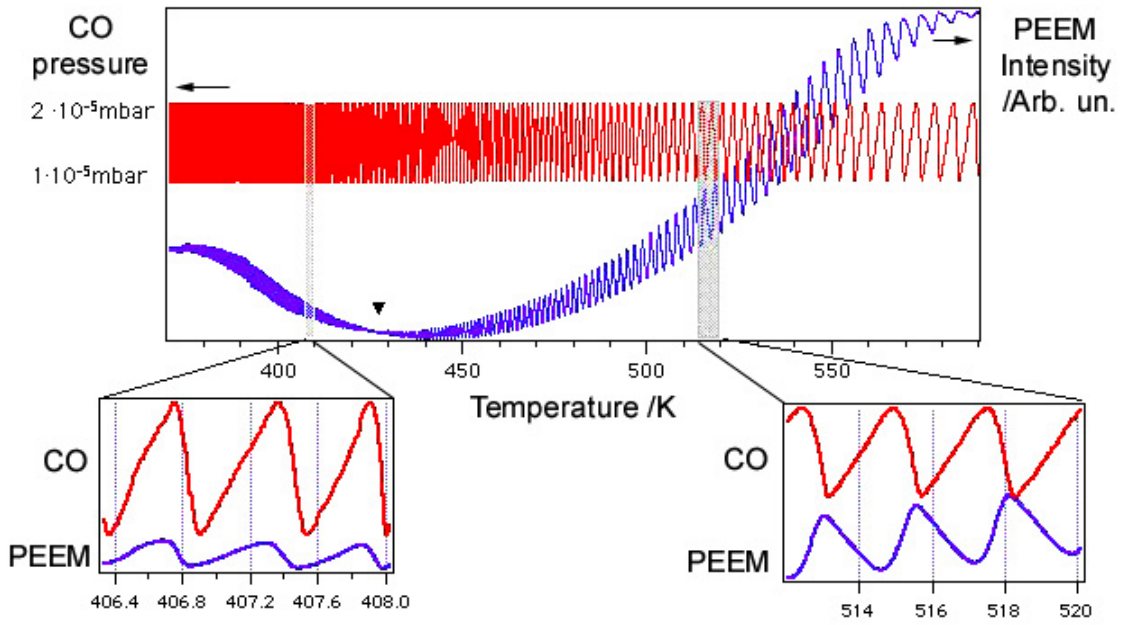

Fig. 3.2 PEEM intensity as a function of the temperature in the presence of an oscillating CO partial pressure. The two insets present details of the phase difference between CO pressure and PEEM intensity.

3.1 Introduction to the Thermal Desorption Spectroscopy (TDS)

The thermally-induced desorption of adsorbates is one of the central aspects of the gas-solid interactions at interfaces. The desorption event of a single particle takes place when the required amount of energy to leave the surface is transferred to the adsorbate. From an investigation of a large ensemble of particles desorbing from a surface we can yield information on the interaction between a single particle and the solid. So far, thermal desorption seems to be a simple experiment with a simple interpretation. Interpretation and analysis have been performed on the basis of a thermally activated process, as described by Arrhenius kinetics [6]. However, deviations between mathematically predicted desorption behavior and observed desorption rates were often found. The cause is that adsorbed particles may experience different energy barriers according to the type of adsorption site characteristic of a specific ordered structure of the adsorbate on the surface. The structure, in turn, depends on the overall coverage of the adsorbate on the surface. Additionally, particle-particle interactions, direct or surface-mediated, can affect the desorption energy threshold.

To cope this complex scenario, two major variants of mathematical descriptions have been developed to describe desorption processes. The lattice-gas models, which incorporate data from several experimental surface science investigations, take into account all kinds of interactions and structural changes known for the system under consideration [7] [8]. By this approach a complete physical understanding of the system is gained. An alternative description, based on the mean-field approximation, is constructed by the use of additional refinements to the Arrhenius kinetics. Although this neglects to include most of the structural details, the characteristic length scale of the mean-field approach nicely matches the wavelength of the patterns that have been observed in PEEM experiments.

For this reason we favor the description of the desorption process based on the Arrhenius kinetics. We will explain how the latter is going to be modified by taking into account structural changes of the adsorbate layer and molecule-molecule interactions. Further refinements, dealt with in the statistical models, have not been considered.

The pattern formation in the CO oxidation on Pt(110) has been successfully described by mean-field models [9] [10] [11] with a good qualitative agreement between experiments and modeling. Quantitative agreements rely, however, on a correct description of several elementary processes such as the desorption of CO, for which an appropriate accuracy has not yet been achieved. For example, the reported coverage dependence of the desorption rate has been rarely incorporated into the modeling.

The rest of the chapter describes an experiment of CO thermal desorption from Pt(110) by means of mass spectroscopy (QMS) and photoemission electron microscopy (PEEM). The desorption rate was assumed to follow an Arrhenius kinetics. However, a coverage dependence has been allowed for the activation energy and for the pre-exponential factor. Unlike the activation energy, for which a marked coverage dependence was found, the pre-exponential factor is largely independent of the adsorbate surface concentration.

3.2 Facts about the CO adsorption-desorption on Pt(110)

The sticking coefficient follows a precursor kinetics [5]. In the precursor state a molecule experiences a great number of hopping processes, by which it progressively loses the initial translation energy in favor of the phonon modes of the substrate. The value of the sticking coefficient at low coverage (0.8) is largely insensitive to the temperature in the range of 200-600 K [12]. The heat of adsorption of CO on Pt(110) is constant till 0.5 monolayer (160 KJ $\cdot$ mol^{-1}) and shows a 10% decrease at higher coverages [13]. In the zero coverage limit, the values of the pre-exponential factor and activation energy for desorption are $3 \cdot 10^{14}$ s^{-1} and 150 KJ $\cdot$ mol^{-1}, respectively, as reported by several authors [12], [14]. The pre-exponential factor, as already stated, exhibits no substantial coverage dependence [15]. During the growth CO forms islands: the CO-CO interaction is believed to be attractive at low coverages and repulsive at high coverages [16]. Two peaks (at 400 and 520 K) are apparent [17], [12], [16] in the TD spectra at saturation coverage. McCabe and Schmidt [18] reported a dramatic dependence of the CO desorption features on the degree of surface oxidation. However, no later work seems to confirm their findings.

3.3 QMS-TD measurements

Fig. 3.3 shows TD spectra of CO on Pt(110) for various initial coverages. The dosing has been performed at 350 K. Only in one case a lower adsorption temperature (300 K) was chosen to obtain the highest CO coverage. We found the frequently reported behavior. The high coverage adsorption peak (at 390 K) is found only for sufficiently low adsorption temperatures. At higher adsorption temperatures the high coverage state is absent and the maximum coverage is only 0.7. To estimate the contribution of the backside of the sample to the desorption signal, a TD spectrum right after sputtering the CO-saturated Pt surface has been recorded. Less than 5% of the signal was comparatively obtained.

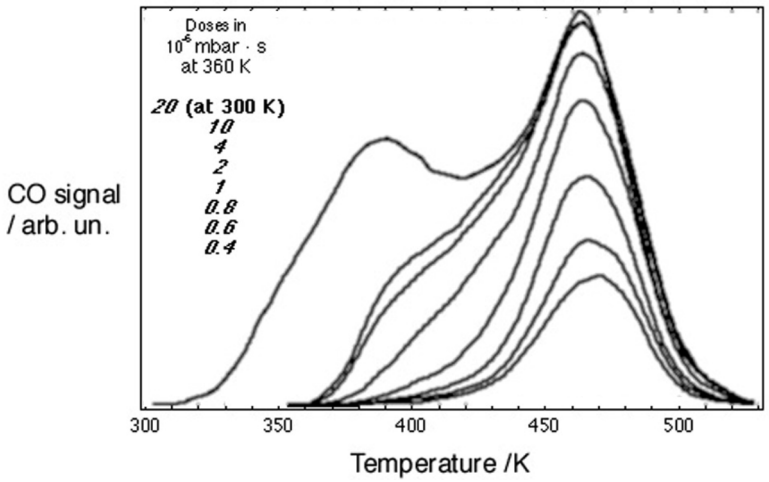

Fig. 3.3 The set of measured TD spectra at different initial CO coverages

As apparent in Fig. 3.3, the position of the CO desorption peaks in the present work are shifted by about 40 K to lower temperatures, compared to the values in the above-mentioned literature. However, variations of several tens of degrees K for the TD peak position are not uncommon for the CO/Pt(110) system (500, 525, and 550 K according to [19], [16], and [18], respectively) and are probably due to the presence of oxide species [18]. The presence of oxides apparently increases the temperature where the TD peak is found. Another aspect is the dependence of the position (T_{Max}) of the maximum of the desorption rate from heating rate (β). A viable way to check the consistency of two sets of results (the present work and reference [12]) characterized by different values of T_{Max} and β (460 K, 6 Ks^{-1} and 510 K, 20 Ks^{-1}, respectively) is to use Eq. 1 [20]:

$$\mathrm{Log}\left(\frac{T_{Max}^2}{\beta}\right) = \mathrm{Log}\left(\frac{E_D}{k_D R}\right) + \frac{E_D}{R}\frac{1}{T_{Max}}. \qquad (1)$$

Since the first term on the right hand side is independent of β and T_{Max} for any set of values the difference between the term on the left and the second on the right side has to yield a constant. However, the comparison of the two values (4.49 and 4.06) does not conclusively prove the compatibility of the two results. Another possibility to explain the differences in the position of the TD peak between the present work and the values reported in literature (e.g. [11]) might be a malfunctioning thermocouple wiring. Broken thermocouple wires that have been indeed repaired a number of times in the course of the experiments could have, in fact, caused misleading temperature readings.

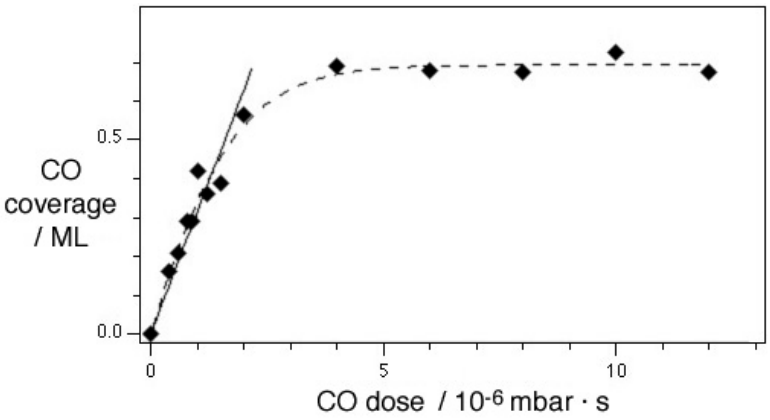

Fig. 3.4 The CO coverage vs. exposure derived from the TD spectra.

The analysis of the TD peak areas for CO deposited at 360 K is plotted in Fig. 3.4. The highest value was used to calibrate the full coverage level of 1 ML. From the peak shape and sizes and by comparing our data with those of Fair and Madix [12] we estimate a maximum CO coverage of 1 ML and an initial sticking coefficient of 1.0, which differs slightly from the values reported in the literature (between 0.65 and 0.8). However, these variations probably reflect only differences in the partial pressure measurement. Variations as high as 20% are common when the readings of different pressure gauges are compared. The problem of absolute coverage determination will be discussed in the following. The characteristic uptake curve is indicated with the dashed line in Fig. 3.4. The sticking coefficient is initially constant, a characteristic of the precursor state. The saturation coverage, 0.7 ML depositing CO at 360 K, reaches 1 ML by dosing CO at temperatures as low as 300 K. This effect is due to the striking difference in the CO desorption at high coverages between 300 and 360 K.

3.4 The mathematical treatment

The kinetics of the CO adsorption can be modeled by an ordinary differential equation [21]:

$$\frac{du}{dt} = k_A\, p_{CO}\, s_{CO} \left(1 - u^3\right). \qquad (2)$$

Here u is the relative CO coverage, p_{CO} the CO partial pressure, s_{CO} the initial CO sticking coefficient; $k_A = 3.14 \cdot 10^5$ ML $\cdot$ mbar^{-1} represents the flux, converted in ML, of CO molecules impinging the surface. The $(1\text{-}u^3)$ term mimics the precursor state kinetics of the CO adsorption.

Rather complex concepts have been applied to describe the desorption process. Detailed approaches, like the one developed by Myshlyavtsev and Zhdanov [8], include several direct and indirect adsorbate-substrate and adsorbate-adsorbate interactions. Here, on the contrary, a simpler model [21] is employed to describe the desorption kinetics of CO from Pt(110) by assuming that the activation energy for desorption $E_D(u)$ depends on the CO coverage due to repulsive CO-CO interactions at high adsorbate densities. The pre-exponential factor k_D^o is assumed to be coverage-independent.

The average desorption rate constant k_D is expressed as a function of the coverage u and the sample temperature T(k_B) is the Boltzmann constant:

$$k_D(u,T) = k_D^o \exp\left(-\frac{E_D(u)}{k_B T}\right). \qquad (3)$$

In the present PEEM experiment the CO coverage at equilibrium for different CO pressures has been recorded, yielding isotherm u(p_{CO}) curves. We assume that the CO coverage u follows to the following equation:

$$\frac{du}{dt} = k_A\, p_{CO}\, s_{CO}\, (1 - u^3) - k_D(u,T)\, u. \qquad (4)$$

When the equilibrium between CO adsorption and desorption is reached, du/dt equals to zero. Eq. (4) can then be rearranged to yield an expression for k_D(u,T):

$$k_D(u,T) = \frac{k_A\, p_{CO}\, s_{CO}\, (1 - u^3)}{u}. \qquad (5)$$

3.5 The PEEM-TD experiment

Fig. 3.5 shows a series of curves recorded with PEEM. From previous results it is known that the PEEM image intensity is strictly proportional to the CO coverage with

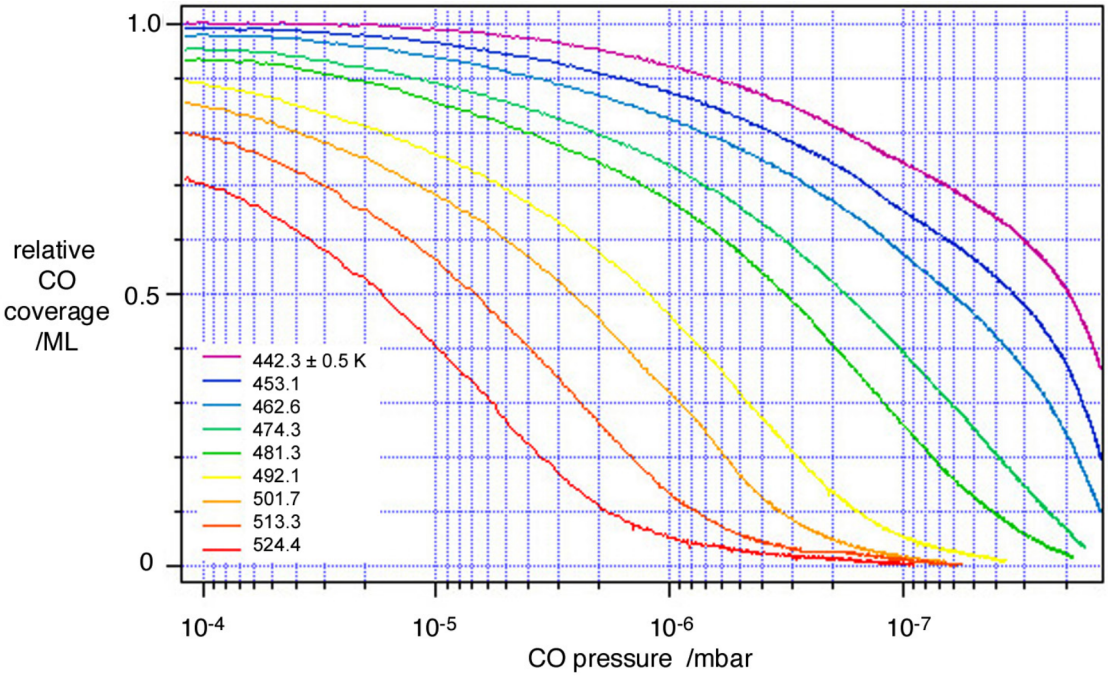

Fig. 3.5 PEEM isotherms.

a negative proportionality factor [22].

The intensity axis only needed to be inverted and “0” and “1” were used to designate the minimum and maximum coverages. In the case of the minimum coverage there is evidently no error. The value for the maximum coverage, however, has to be taken as relative. The relative coverage of 1 is defined as the saturation coverage at 442 K and at a CO partial pressure of $1 \cdot 10^{-4}$ mbar.

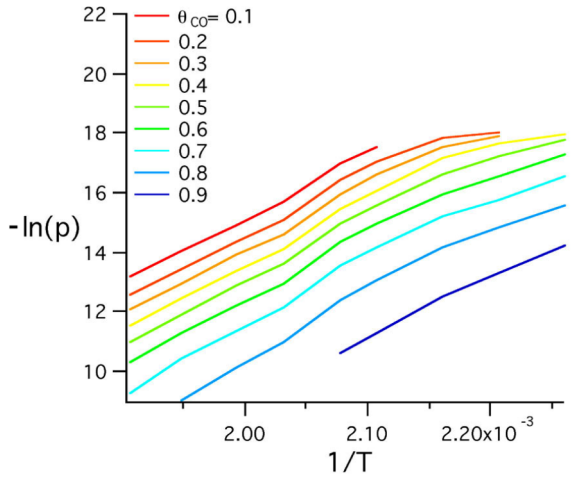

Fig. 3.6 PEEM isocores.

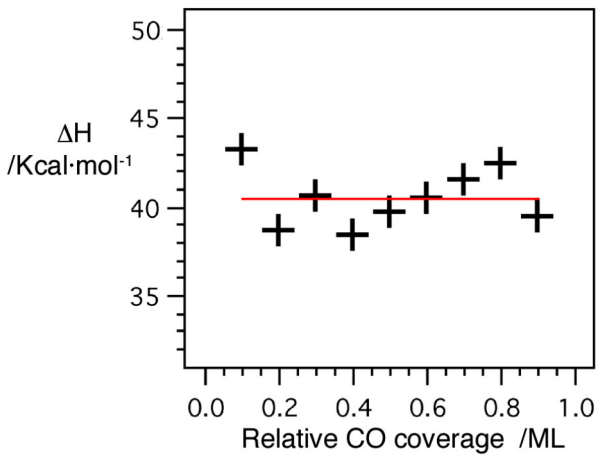

Fig. 3.7 The values of ΔH as derived by Eq. (6).

The PEEM isotherm, arranged to yield the isocores shown in Fig. 3.6, can be used to calculate the enthalpy change of the process by the Clausius-Clapeyron equation:

$$\frac{d\ \ln p}{d\,1/T} = -\frac{\Delta H}{R}. \qquad (6)$$

The results are displayed in Fig. 3.7. By identifying the enthalpy change with the activation energy for desorption, we get a first estimate for the latter of about 41 ± 2 Kcal · mol^{-1} in the limit of zero coverage. This evaluation is valid as far as the entropy term, proportional to the logarithm of the pressure difference in the system, is negligibly small.

The data of $u(p_{CO})$ in Fig. 3.5 can be transformed by Eq. (5) to yield curves of $k_D(u,T)$ as displayed in Fig. 3.8. By using the constrain on the behavior of $k_D(u,T)$, we can now extract k_D^o and $E_D(u)$ from the $k_D(u,T)$ curves. This is done by transforming Eq. (3) to the form of:

$$-k_B T\ \ln(k_D(u,T)) + k_B T \ln(k_D^o) = E_D(u). \qquad (7)$$

The first term of the left-hand side is fully determined and yields the coverage dependent part of $E_D(u)$. The fact that $E_D(u)$ is independent of the temperature is then used to find the best fit of k_D^o.

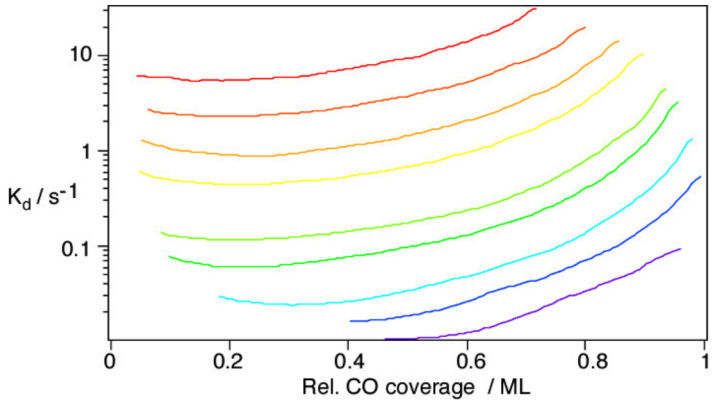

Fig. 3.8 Desorption constant as a function of coverage for different temperatures.

The resulting curves of $E_D(u)$ are displayed in Fig. 3.9. The solid lines show the results for each of the curves of Fig. 3.8. The dotted lines correspond to the average and a fit of the data. The resulting initial activation energy and pre-exponential factor are 40.9 ± 0.5 Kcal · mol^{-1} and $7 \cdot 10^{17\pm1}$ ML · s^{-1}, respectively.

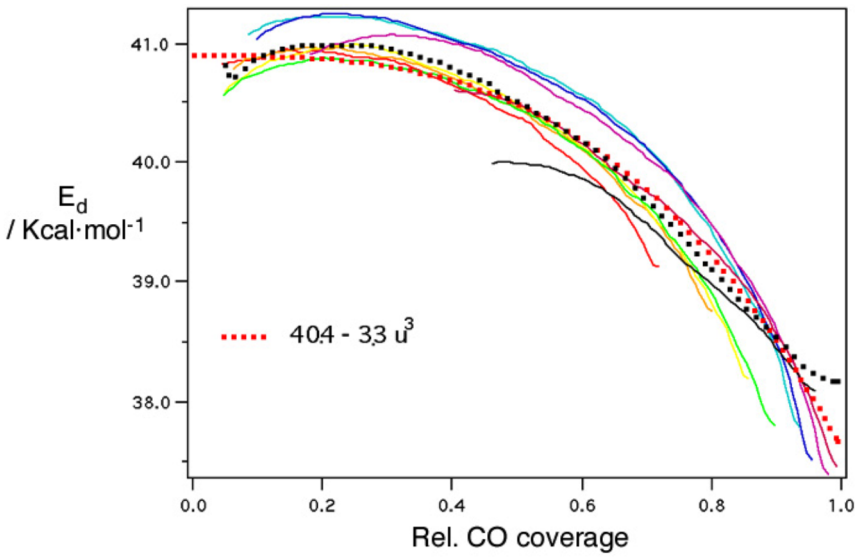

Fig. 3.9 Desorption energy vs. coverage.

These results can be used to simulate desorption spectra. Eq. (4) is numerically integrated, starting with different initial relative coverages from 0 to 1 and without adsorption (p_{CO}=0). The simulated curves, shown in Fig. 3.10, manifest two important features. First, their peaks are found at different temperatures compared to the dynamical measurement during a thermal desorption experiment. This discrepancy, already discussed above and ascribed to malfunctioning thermocouple wiring, did not occur in the measurements at the thermal equilibrium. Furthermore, the simulated curve for a relative coverage of 1 seems to be equivalent with experimental TD curves with an absolute coverage of 0.7 ML (see Fig. 3.3 or reference [12]). This is an important step to bring simulations close to the real experimental conditions. In fact, up to now in the simulations of the CO oxidation model it has been overlooked that around 500 K and CO partial pressures of 10^{-4} mbar no coverage greater than 0.6 ML is possible. The value of 0.6 ML is derived from the maximum relative coverage that is 85 % at 500 K (see Fig. 3.4) multiplied by 0.7.

At this point, the cited work of Myshlyavtsev and Zhdanov [8] helps to understand the experimental and the simulated CO desorption data. They found a step-like behavior for the activation energy as a function of the CO coverage and calculated that above 0.5 ML the activation energy drops abruptly by about 8 Kcal/mol.

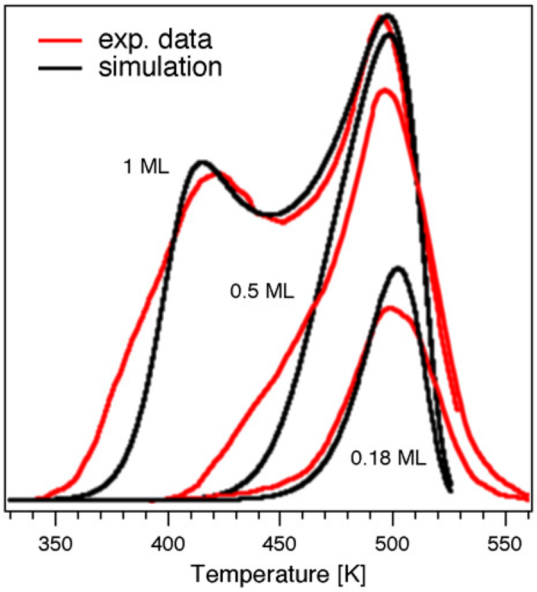

Fig. 3.10 Experimental and simulated TD spectra.

Fig. 3.10 shows a comparison between the measured TD data for initial coverages of 0.18, 0.5, and 1.0 ML and the simulated TD curves with the same initial coverages. To allow a direct comparison with the results of the simulation the experimental TD spectra have been shifted by 40 K to higher temperatures. For the coverage-dependent activation energy of desorption a step function of the following form was used:

$$E_D(u) = \frac{(E_0 + E_1)}{2} - \frac{(E_0 - E_1)}{2} \tanh\left(\frac{u - u_s}{\delta}\right). \qquad (8)$$

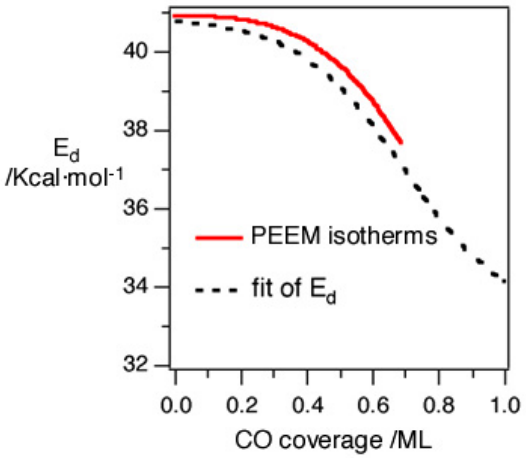

Fig. 3.11 The desorption energy vs. the CO coverage.

E_0 and E_1 are the activation energies characteristic of the two plateaus, u_s corresponds to the critical CO coverage, and δ takes into account the particular form of the energy drop. The activation energy of desorption at low CO coverage has been already determined: E_0= 40.9 Kcal/mol. The values of u_s and δ had to satisfy the coverage dependence in the interval $0 < u < 0.6$. Eventually, the least square fitting of E_1, δ and u_s yields the dotted curve displayed in Fig. 3.11. The best fit was obtained for the following values:

$$k_D^o = 7.2 \cdot 10^{17} \text{ ML/s}$$
$$E_0 = 40.9 \text{ kcal/mol}$$
$$E_1 = 33.2 \text{ kcal/mol}$$
$$u_s = 0.69, \delta = 0.32.$$

The conclusion is that indeed the PEEM integrated intensity of a CO covered Pt(110) surface can be successfully employed as a measure of the adsorbate coverage, although some precautions have to be taken concerning the heating rate and the position of the maxima of the desorption peaks. This result will be used in the following chapters, dealing with CO desorption phenomena.

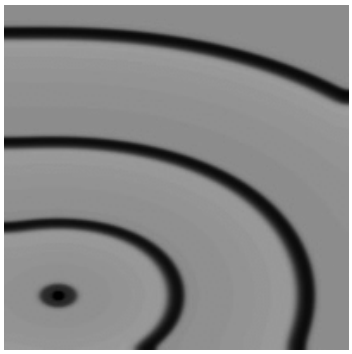

Fig. 3.12 Simulation of a target pattern: oxygen waves spread through the CO sea: $p_{CO} = 2.8 \cdot 10^{-5}$, $p_{CO} = 2 \cdot 10^{-4}$, T = 480 K; image: 200 x 200 μm^2.

Moreover, the resulting kinetic values have been inserted in the *virtual lab* code, written by A. v. Oertzen and used to perform simulations of the spatio-temporal pattern evolution in the CO oxidation. An example is shown in Fig. 3.12. On a CO-covered surface a small area is artificially kept at high oxygen coverage. This *defect* acts as nucleation center for target waves. Thanks to the newly derived values for the CO desorption it has been possible to bring that kind simulation closer to the actual experimental condition. The value of the simulated temperature, at which target patterns appear, is in fact now just a few degrees higher than in the real experiments.

The next two chapters deal with further features associated with the CO oxidation on the Pt(110) surface, namely the formation of subsurface oxygen and the surface reconstruction. Both phenomena play a role in the description of the pattern formation in the CO oxidation, account for nonlinear kinetic effects, and are not fully understood.

[1] N. Freyer, M. Kiskinova, G. Pirug, and H. P. Bonzel, *Site-specific core level spectroscopy of CO and NO adsorption on Pt(110) (1x2) and (1x1) surfaces*, Appl. Phys. A **39**, 209 (1986).

[2] R. Imbihl, S. Ladas, and G. Ertl, *The CO-induced 1x2-1x1 phase transition of Pt(110) studied by LEED and work function measurements*, Surf. Sci. **206**, L903 (1988).

[3] R. Imbihl (Private communications).

[4] R. M. Eiswirth, *Phänomene der Selbstorganisation bei der Oxidation von CO an Pt(110)*, Ph. D. thesis, Technische Universität München, 1987.

[5] C. M. Comrie and R. M. Lambert, *Chemisorption and surface structural chemistry of CO on Pt(110)*, J. Chem. Soc. Farad. Trans. 1 **72**, 1659 (1975).

[6] T. L. Hill, *Statistical mechanics* (McGraw-Hill, New York, 1956).

[7] S. J. Lombardo and A. T. Bell, Surf. Sci. Rep. **13**, 1 (1991).

[8] A. V. Myshlyavtsev and V. P. Zhdanov, *Surface reconstruction and thermal desorption: the missing-row model for CO/Pt(110)*, Langmuir **9**, 1290 (1993).

[9] K. Krischer, M. Eiswirth, and G. Ertl, *Oscillatory CO oxidation on Pt(110): Modeling of temporal self-organization*, J. Chem. Phys. **96**, 9161 (1992).

[10] M. Bär, C. Zülicke, M. Eiswirth, and G. Ertl, *Theoretical modeling of spatiotemporal self-organization in a surface catalyzed reaction exhibiting bistable kinetics*, J. Chem. Phys. **96**, 8595 (1992).

[11] A. v. Oertzen, A. Mikhailov, H. H. Rotermund, and G. Ertl, *Subsurface oxygen formation on the Pt(110) surface: Experiments and mathematical modelling*, Surf. Sci. **350**, 259 (1996).

[12] J. Fair and R. J. Madix, *Low and high coverage determinations of the rate of carbon monoxide adsorption and desorption from Pt(110)*, J. Chem. Phys. **73**, 3480 (1980).

[13] T. E. Jackman, J. A. Davies, D. P. Jackson, W. N. Unertl, and P. R. Norton, *The Pt(110) phase transition: a study by Rutherford backscattering, nuclear microanalysis, LEED and Thermal Desorption Spectroscopy*, Surf. Sci. **120**, 389 (1982).

[14] J. R. Engstrom and W. H. Weinberg, *Analysis of gas-surface reactions by surface temperature modulation: experimental applications to the adsorption and oxidation of carbon monoxide on the Pt(110)-(1x2) surface*, Surf. Sci. **201**, 145 (1988).

[15] E. Seebauer, A. Kong, and L. Schmidt, *The coverage dependence of the pre-exponential factor for desorption*, Surf. Sci. **193**, 417 (1988).

[16] P. Hofmann, S. R. Bare, and D. A. King, *Surface phase transitions in CO chemisorption on Pt(110)*, Surf. Sci. **117**, 245 (1982).

[17] H. P. Bonzel and R. Ku, *Mechanism of the catalytic carbon monoxide oxidation on Pt(100)*, Surf. Sci. **33**, 91 (1972).

[18] R. W. McCabe and L. D. Schmidt, *Adsorption of H2 and CO on clean and oxidized Pt(110)*, Surf. Sci. **60**, 85 (1976).

[19] R. M. Lambert and C. M. Comrie, *The oxidation of CO by NO on Pt(111) and Pt(110)*, Surf. Sci. **46**, 61 (1974).

[20] K. Christmann, *Introduction to Surface Physical Chemistry* (Steinkopff-Verlag, Darmstadt, 1991).

[21] M. Eiswirth and G. Ertl, *Kinetic oscillations in the catalytic CO oxidation on a Pt(110) surface*, Surf. Sci. **177**, 90 (1986).

[22] A. v. Oertzen, H. H. Rotermund, and S. Nettesheim, *Diffusion of carbon monoxide and oxygen on Pt(110): experiments performed with the PEEM*, Surf. Sci. **311**, 322 (1994).